

**23rd International Conference on
Harmonisation within Atmospheric Dispersion Modelling
for Regulatory Purposes
15-19 September 2025, Hamburg, Germany**

EXTENDED ABSTRACT

***A new parameterization of CFD boundary conditions reproducing the Ekman spiral
under stable atmospheric conditions***

Youness El-Ouartassy¹

youness.el-ouartassy@enpc.fr / y.elouartassy@gmail.com

Martin Ferrand¹, Eric Dupont¹ and Guilhem Balvet¹

¹CEREA, EDF R&D, École nationale des ponts et chaussées, 78400 Chatou, France

Abstract: This work focuses on a crucial issue for CFD simulations of atmospheric pollutant dispersion at local scale: the robustness of inlet boundary conditions. Using a generalized Nieuwstadt (1984) theory (valid only under stably stratified conditions), new parameterizations that are more general than those used to date (typically based on Monin-Obukhov similarity theory) are derived, continuously blending the Monin-Obukhov surface layer and Ekman spiral. The developed formulations are implemented in the CFD solver code `_saturne`. Then, preliminary results of using these profiles as inlet boundary conditions to calculate atmospheric dispersion are presented and compared with measurements from the Prairie Grass field experiment.

Key words: Stable condition, Nieuwstadt theory, Universal functions, Ekman spiral, Boundary layer profiles, CFD, code `_saturne`.

Introduction

Today, Computational fluid dynamics (CFD) is used in various contexts, such as atmospheric pollutant dispersion and environmental studies, for local-scale modelling of atmospheric boundary layer (ABL) dynamics. This approach is based on solving the Reynolds-averaged Navier-Stokes (RANS) equations and other conservation equations to accurately represent the physical processes involved in atmospheric flow, particularly the turbulence. However, the accuracy of CFD simulations depends closely on the representativeness of the boundary conditions imposed, in particular wind speed and potential temperature profiles, which are the two key variables affecting atmospheric turbulence.

A classical approach to build generic inlet profiles is to use Monin-Obukhov similarity theory (MOST) to derive so called “*universal functions*”, from which all near-surface turbulent flow quantities can be derived considering idealized situations: homogenous horizontal flow in a steady state, with a constant shear $\overline{u'w'}$ (as a function of the friction velocity u_{*0}) and a constant heat flux $\overline{w'\theta'}$ (as a function of the friction velocity u_{*0} and temperature θ_{*0}). Beyond the surface layer, the assumptions underlying this similarity theory break down due to the influence of the *Coriolis force* effect and *larger-scale turbulent eddies*, leading to significant inaccuracies.

This limitation highlights the importance of developing and employing boundary conditions that account for the full vertical structure of the ABL, blending the Monin-Obukhov surface layer and Ekman spiral. In this context, the work presented here aims to extend the Nieuwstadt (1984) theory (based on second-order moment turbulent closures) in order to derive universal functions that are able to reproduce the Ekman spiral in stably stratified atmospheres.

**23rd International Conference on
Harmonisation within Atmospheric Dispersion Modelling
for Regulatory Purposes
15-19 September 2025, Hamburg, Germany**

Derivation of theoretical profiles

Nieuwstadt (1984) theory in a few words

Within the framework of Nieuwstadt theory, the atmospheric flow is still assumed to be in a steady state and horizontally homogenous, as for the MOST. However, Coriolis force effect is taken into account, a large-scale pressure gradient is considered by imposing a geostrophic wind, and a production-dissipation equilibrium is assumed for the turbulent kinetic energy (TKE) transport equation: $P + B - \varepsilon = 0$, where P , B and ε are, respectively, the TKE production by the shear, the TKE production by buoyancy and the TKE dissipation rate. Furthermore, in stable situations, above the surface layer, the gradient and flux Richardson numbers (Ri and Ri_f , respectively) are assumed to have reached constant critical values. Finally, a radiative source term S in the Reynolds-averaged energy equation is added as a constant function of height. Injecting all these assumptions into the second-order turbulence model of Brost and Wyngaard (1978) (later called BW78), Nieuwstadt (1984) derived vertical profiles for the mean velocity components (\bar{u} , \bar{v}) and mean temperature $\bar{\theta}$.

Generalized Nieuwstadt (1984) profiles

In this work, the profiles derived by Nieuwstadt (1984) are generalized in two ways following Ferrand et al. (2025). The first one by considering the radiative source term in the temperature equation as a power law of the height:

$$S = u_{*0} \theta_{*0} \frac{\alpha}{z_i} \left(1 - \frac{z}{z_i}\right)^{\alpha-1} \quad (1)$$

where z_i is the ABL height and α is a dimensionless exponent. The later is taken to be 1 in Nieuwstadt (1984). However, in order to be as general as possible, in a first time, we let α without specifying a value. Then, we demonstrate that, under Nieuwstadt theory assumptions mentioned above, the momentum RANS equations have a solution if the height of the ABL satisfies the following criterion:

$$z_i = \sqrt{\frac{\sqrt{\alpha(\alpha+2)}}{2}} (\alpha+1) \kappa Ri_f^c \times \sqrt{\frac{u_{*0} L_{MO}}{|f|}} \quad (2)$$

where $\kappa \approx 0.4$ is the Von Karman constant, $Ri_f^c = 0.25$ is the critical flux Richardson number value, f is the Coriolis parameter, and $L_{MO} = \frac{u_{*0}^2 \theta_0}{\kappa g \theta_{*0}}$ is the Obukhov length scale, which is defined as the ratio of the shear and buoyant effects.

Finally, aligning the x -axis with ground wind direction, we obtain algebraic solutions for mean wind components and mean potential temperature profiles in function of the flux Richardson number Ri_f , respectively, as:

$$\frac{\partial \bar{u}}{\partial z} = \frac{u_{*0}}{\kappa L_{MO} Ri_f} \left(1 - \frac{z}{z_i}\right)^{\frac{\alpha}{2}-1} \cos\left(\frac{\sqrt{\alpha(\alpha+2)}}{2} \ln\left(1 - \frac{z}{z_i}\right)\right) \quad (3)$$

$$\frac{\partial \bar{v}}{\partial z} = \frac{u_{*0}}{\kappa L_{MO} Ri_f} \left(1 - \frac{z}{z_i}\right)^{\frac{\alpha}{2}-1} \sin\left(\frac{\sqrt{\alpha(\alpha+2)}}{2} \ln\left(1 - \frac{z}{z_i}\right)\right) \quad (4)$$

$$\frac{\partial \bar{\theta}}{\partial z} = \frac{\theta_{*0}}{\kappa L_{MO}} \frac{Ri}{Ri_f^2} \left(1 - \frac{z}{z_i}\right)^{\alpha-2} \quad (5)$$

In order to avoid the problem of singular profiles at the junction with the free atmosphere (i.e, at $z = z_i$), we can see that the exponent parameter α must be greater than 2.

According to the Nieuwstadt theory, the gradient and flux Richardson numbers in the wind speed and temperature distributions (Eqs. 3 – 5) are assumed to be constants above the surface layer.

**23rd International Conference on
Harmonisation within Atmospheric Dispersion Modelling
for Regulatory Purposes
15-19 September 2025, Hamburg, Germany**

Thus, the second ingredient to extend these profiles is to use the Richardson numbers as local parameters. To this end, in a first step, we rewrite Ri_f in function of the Monin-Obukhov momentum and heat universal functions (respectively, $\varphi_m = \frac{\kappa z}{u_*} \frac{\partial \bar{U}}{\partial z}$ and $\varphi_h = \frac{\kappa z}{\theta_*} \frac{\partial \bar{\theta}}{\partial z}$) as follows:

$$Ri_f = -\frac{B}{P} = \frac{\zeta}{\varphi_m(\zeta)} \quad (6)$$

with $\zeta = \frac{z}{L_{MO}}$ is the dimensionless parameter characterising the overall dynamic and thermal processes in the surface layer.

Then, using the set of turbulence equations of BW78, used by Nieuwstadt (1984), we can express Ri in function of Ri_f , which formally makes appear the turbulent Prandtl number $Pr_t = \frac{Ri}{Ri_f}$:

$$Ri = \frac{d \left[(1 - C_2)(W_0(1 - Ri_f) + W_1) - \frac{C_1}{2}(1 - Ri_f) \right] - (1 - a_2)(1 + C_3)Ri_f}{(1 + C_3)Ri_f + C \left[W_0(1 - Ri_f) + W_1 - \frac{1 - a_1}{C_\theta} Ri_f \right]} \times Ri_f \quad (7)$$

with the following constants: $C = 6$, $C_1 = 0.207$, $C_2 = 0.1$, $C_3 = -0.8$, $d = 9.7$, $C_\theta = 1.4$, $a_1 = 0.5$, $a_2 = 0.5$, $W_0 = \frac{1}{3} + \frac{4(1+C_3)}{3c}$, and $W_1 = \frac{2(C_2 - 2C_3)}{3c} - \frac{2}{c}$. We can see that for a flux Richardson number of zero (i.e, at ground surface), we get: $Pr_t^0 = \frac{d}{c} \left[(1 - C_2) - \frac{C_1}{2(W_0 + W_1)} \right] \approx 0.73$.

The use of the presented extended formulations of Ri and Ri_f into the equations of wind speed and temperature allows a continuous blending of the surface layer and Ekman spiral: in the surface layer, for $z \ll z_i$ (and then $1 - z/z_i \sim 1$), the same profiles as the MOST are produced.

Boundary-law at ground surface

The use of the classical transport equation (typically used for first-order closures) for the TKE dissipation rate ε , which includes in its diffusion term $\left(= \frac{\partial}{\partial z} \left(\frac{C_\mu k^2}{\sigma_\varepsilon \varepsilon} \frac{\partial \varepsilon}{\partial z} \right) \right)$ the constants $C_\mu = 0.09$ and $\sigma_\varepsilon = 1.30$, too restrictive compared with the second-order approaches employed here, led to modelling errors, particularly near the ground. Indeed, algebraic closures give $\frac{\overline{u'w'}}{k} \sim \sqrt{C_\mu}$. Thus, these errors are linked to inadequately initiated vertical shear for a given TKE. In order to derive a new values of C_μ and σ_ε consistent with second-order turbulence closures, we consider that atmospheric flow conditions near the ground are equivalent to neutral conditions, which means that $\lim_{z \rightarrow 0} \varphi_m = 1$ and $\lim_{z \rightarrow 0} Ri_f = 0$. These assumptions enable to obtain the following second order model-consistent parametrisations of C_μ and σ_ε :

$$C_\mu = \frac{4(W_0 + W_1)(1 - C_2)}{c} \approx 0.14 \quad \text{and} \quad \sigma_\varepsilon = \frac{\kappa^2}{\sqrt{C_\mu(C_{\varepsilon 2} - C_{\varepsilon 1})}} \approx 0.982 \quad (8)$$

with $C_{\varepsilon 1} = 1.44$, and $C_{\varepsilon 2} = 1.92$ taken from Launder and Spalding (1972).

Validation of derived profiles

Simulations set-up

The algebraic profiles derived are implemented in the CFD solver code `_saturne` and used as inlet boundary conditions. The stability condition is considered with an Obukhov length $L_{MO} = 50m$, and the power exponent parameter is $\alpha = 2.5$. At the top of ABL ($z = z_i$), a constant wind speed is considered, which equal to the geostrophic wind speed. In addition, we use the Höglström (1988) in the expressions of φ_m and φ_h , and we add dissipation terms in second-order turbulent moments for $z > z_i$. Furthermore, the thermal source term (Eq. 1) and Coriolis force are taken into account. The criterion considered for evaluating the profiles is their spatial and temporal conservation along a calculation domain representative of local scales. Thus, two simulations were carried out

**23rd International Conference on
Harmonisation within Atmospheric Dispersion Modelling
for Regulatory Purposes
15-19 September 2025. Hamburg, Germany**

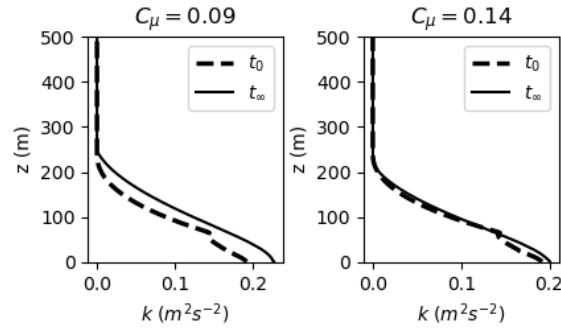


Fig. 1: Comparison of the initial profile and convergence profile of TKE using $C_\mu = 0.09$ (left panel) and $C_\mu = 0.14$ (right panel).

until a quasi-steady state is reached (24h): the first one using a bi-periodic 1D mesh (equivalent to an infinite domain) of $2km$ of height to assess temporal conservation, and the second one using a cylindrical domain of $2km$ of height and $10km$ of diameter to assess spatial conservation.

Results

First, we evaluate the impact of the value of C_μ on the conservation of derived profiles in the case of 1D simulation. To this end, Fig. 1 presents a comparison of TKE profiles using $C_\mu = 0.09$, as defined in the standard $k - \varepsilon$ model, and using the new parameterization that gives $C_\mu = 0.14$. We therefore see that using a C_μ consistent with the second-order closures of the turbulence considered here corrects significantly ground errors that arise between the initial profile and the convergence profile when using a standard C_μ .

Then, in order to evaluate the spatial conservation of profiles, they are compared at $0km$ (inlet), $2km$, $4km$, $6km$, $8km$, and $10km$, as shown in Fig. 2. This result shows a good conservation throughout the simulation domain. In addition, the wind profiles constructed provide an effective modelling of the rotation of the wind along the Ekman spiral.

Application to atmospheric dispersion simulation: preliminary results

The parameterisations developed are used to calculate the atmospheric dispersion of a passive release using a Eulerian approach (code_saturne). Furthermore, an additional dispersion simulation was carried out using a Gaussian approach by implementing an analytical Gaussian solution based on the calculation of Pasquill stability classes. These simulations are then compared to observations from a basis of 10 experimental Prairie Grass emissions, representing various situations of stable ABL conditions.

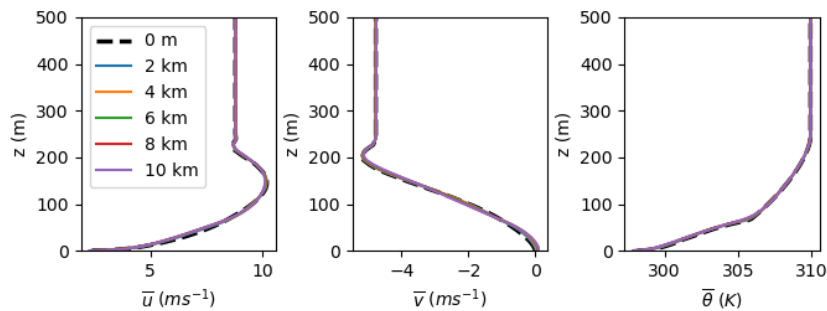


Fig. 2: Conservations of the generalized Nieuwstadt profiles throughout the cylindrical domain (left: \bar{u} ; middle: \bar{v} ; right: $\bar{\theta}$).

**23rd International Conference on
Harmonisation within Atmospheric Dispersion Modelling
for Regulatory Purposes
15-19 September 2025, Hamburg, Germany**

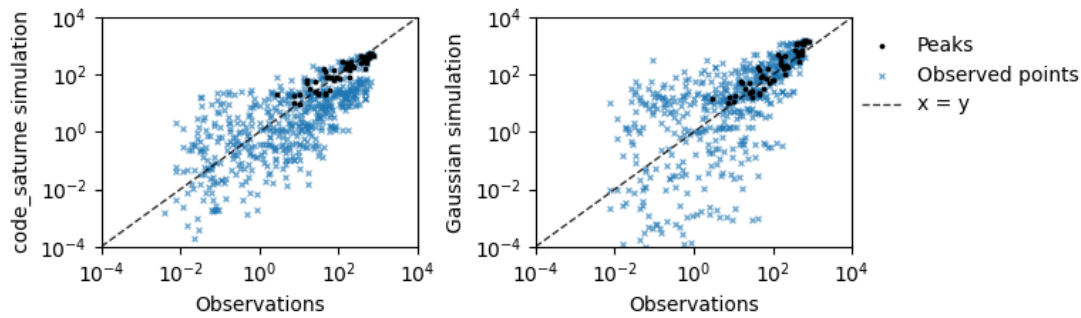


Fig. 3: Scatter plot of the simulated versus experimentally observed concentrations (ppm-mass) at observation arcs for the 10 selected Prairie Grass experiments.

Fig. 3 shows a preliminary result of model-to-data comparison of the dispersion simulations carried out in all observed points. On one hand, it can be seen that peak concentrations were generally well reproduced by both modelling approaches. On the other hand, we can see that the Eulerian approach is slightly more efficient than the Gaussian simulation. However, this result remains qualitative and requires confirmation by calculating statistical indicators.

Conclusions and perspectives

This work presents an extension of Nieuwstadt theory, based on second-order closures of turbulence, in order to derive theoretical profiles of velocity, temperature and turbulence. These profiles have the advantage of taking into account the Coriolis force and the height of the ABL. In addition, a new parameterisation of the C_μ constant consistent with second-order approaches has been developed in order to reduce the persistent errors in the first cells near to the ground. The profiles developed were then implemented in the CFD solver code_saturne and their conservation was validated. Finally, they were used as inlet boundary conditions to simulate short-range atmospheric dispersion. The model-to-data comparison of these simulations, within the framework of the Prairie Grass experiments, showed good performance.

As a perspective, it would be interesting to develop a range of statistical scores to evaluate the quality of the dispersion simulations carried out. In addition, further investigations are required in the case of convective situations where the Nieuwstadt theory no longer holds.

References

- Brost, R. A. and Wyngaard, J. C. (1978). Model Study of the Stably Stratified Planetary Boundary Layer. *Journal of the Atmospheric Sciences*, 35(8):1427–1440.
- Ferrand, M. and Pennel, R. and Dupont, E. (2025). Universal Functions with Ekman spiral and Monin–Obukhov Surface Layers. *Boundary Layer Meteorology*. accepted.
- Launder, B. and Spalding, D. (1974). The numerical computation of turbulent flows. *Computer Methods in Applied Mechanics and Engineering*, 3(2):269–289.
- Monin, A. S. and Obukhov, A. M. (1954). Basic laws of turbulent mixing in the surface layer of the atmosphere. *Contrib. Geophys. Inst. Acad. Sci, USSR*, 151(163):e187.
- Nieuwstadt, F. T. (1984). The turbulent structure of the stable, nocturnal boundary layer. *Journal of Atmospheric Sciences*, 41(14):2202–2216.